Kinetic Isotope Effect Analysis of the Ribosomal Peptidyl Transferase Reaction†

Amy C. Seila,‡ Kensuke Okuda,§,|| Sara Núñez,⊥ Andrew F. Seila,# and Scott A. Strobel*,||

Contribution from the Department of Molecular Biophysics and Biochemistry, Yale University, New Haven, Connecticut 06520-8114

Received October 22, 2004; Revised Manuscript Received December 20, 2004

ABSTRACT: The ribosome is the macromolecular machine responsible for protein synthesis in all cells. Here, we establish a kinetic framework for the 50S modified fragment reaction that makes it possible to measure the kinetic effects that result from isotopic substitution in either the A or P site of the ribosome. This simplified peptidyl transferase assay follows a rapid equilibrium random mechanism in which the reverse reaction is nonexistent and the forward commitment is negligible. A normal effect (1.009) is observed for ^{15}N substitution of the incoming nucleophile at both low and high pH. This suggests that the first irreversible step is the formation of the tetrahedral intermediate. The observation of a normal isotope effect that does not change as a function of pH suggests that the ribosome promotes peptide bond formation by a mechanism that differs in its details from an uncatalyzed aminolysis reaction in solution. This implies that the ribosome contributes chemically to catalysis of peptide bond formation.

The ribosome is the ribonucleoprotein complex responsible for protein synthesis in all cells. The *Escherichia coli* ribosome is a 2.5 MDa enzyme consisting of 3 RNA molecules and 52 proteins. The ribosome catalyzes peptide bond formation, a polymerization reaction in which messenger RNA (mRNA) serves as the template and aminoacylated transfer RNAs (tRNAs) serve as the substrates.

Binding to and stabilizing the transition state (TS) in preference to either the substrate or product is a fundamental strategy employed by enzymes to promote chemical reactions (*1*). Because the catalytic power of an enzyme comes from the interaction of enzyme and TS structures, defining the peptidyl transferase TS is essential to understanding how the ribosome enhances the rate of peptide bond formation. The most definitive approach to characterize the TS is the measurement of kinetic isotope effects (KIEs)[1] (*2*−*5*). Changes in the reaction rate upon isotopic substitution arise from changes in vibrational states between the ground state and TS in a chemical reaction (*6*). The magnitude of the isotope effect is related to the change in bonding to the isotopic atom as the reaction proceeds. Consequently, KIEs provide information necessary to predict the TS of chemical reactions, including those catalyzed by enzymes (reviewed in refs *6*−*11*). A comparison of KIE results for similar catalyzed and uncatalyzed chemical reactions provides information about how an enzyme promotes the chemical reaction.

A KIE can be measured by isotopically labeling reactive functional groups in the substrates and determining the relative reaction rates of the heavy and light substrates by competitive methods, in which labeled and unlabeled substrates are mixed and compete for reaction (*12*). The isotopic ratio can be measured by whole-molecule mass spectrometry, and the KIE can be calculated from the change in isotopic composition of the unreacted starting material over the course of the reaction.

The elongation phase of protein synthesis, in which amino acids are added to the C terminus of a growing polypeptide chain, is a multistep process involving several protein factors. The chemical reaction catalyzed by the peptidyl transferase center consists of attack by the α-amino group of the A-site tRNA on the carbonyl carbon of the P-site tRNA. This reaction results in deacylation of the P-site tRNA and transfer of the growing polypeptide chain onto the A-site tRNA. The mechanism by which the ribosome catalyzes this reaction is a matter of significant interest but remains unresolved.

The first irreversible step must occur after the isotope-sensitive step to measure a KIE; therefore, a full tRNA reaction is not amenable to KIE analysis. It is known from kinetic studies that accommodation of the amino-acyl tRNA into the A site is rate-limiting during the elongation phase of protein synthesis (*13*). Alternatively, a single-turnover assay that utilizes puromycin as the A-site substrate and a prebound tRNA as the P-site substrate has been developed (*14*). This assay avoids rate-limiting accommodation, but it

† This work was supported by NIH Grant GM54839 and an American Cancer Society Beginning Investigator Award to S.A.S.

* To whom correspondence should be addressed. Telephone: (203) 432-5566. Fax: (203) 432-5767. E-mail: strobel@mail.csb.yale.edu.

‡ Department of Genetics, Yale University.

§ Current address: Faculty of Pharmaceutical Sciences, Okayma University, 1-1-1 Tsushima-naka, Okayma 700-8530, Japan.

|| Department of Biochemistry and Biophysics, Yale University.

⊥ Department of Biochemistry, Albert Einstein College of Medicine.

Department of Management Information Systems, University of Georgia.

[1] Abbreviations: KIE, kinetic isotope effect; CCA_N-Phe, cytidylyl-(3′-5′)-cytidylyl-(3′-5′)-N^6,N^6-dimethyladenosyl-3′-amino-3′-deoxy-3′-L-phenylalanine; CCApcb, CC-3′-(biotinyl-ε-aminocaproyl-L-phenylalanyl)A; CCA_N-Phe-pcb, cytidylyl-(3′-5′)-cytidylyl-(3′-5′)-N^6,N^6-dimethyladenosyl-3′-amino-3′-deoxy-3′-L-phenylalanine-L-phenylalanine-caproic acid-biotin; pK_a, acidity constant.

10.1021/bi047742f CCC: $30.25
Published on Web 02/16/2005

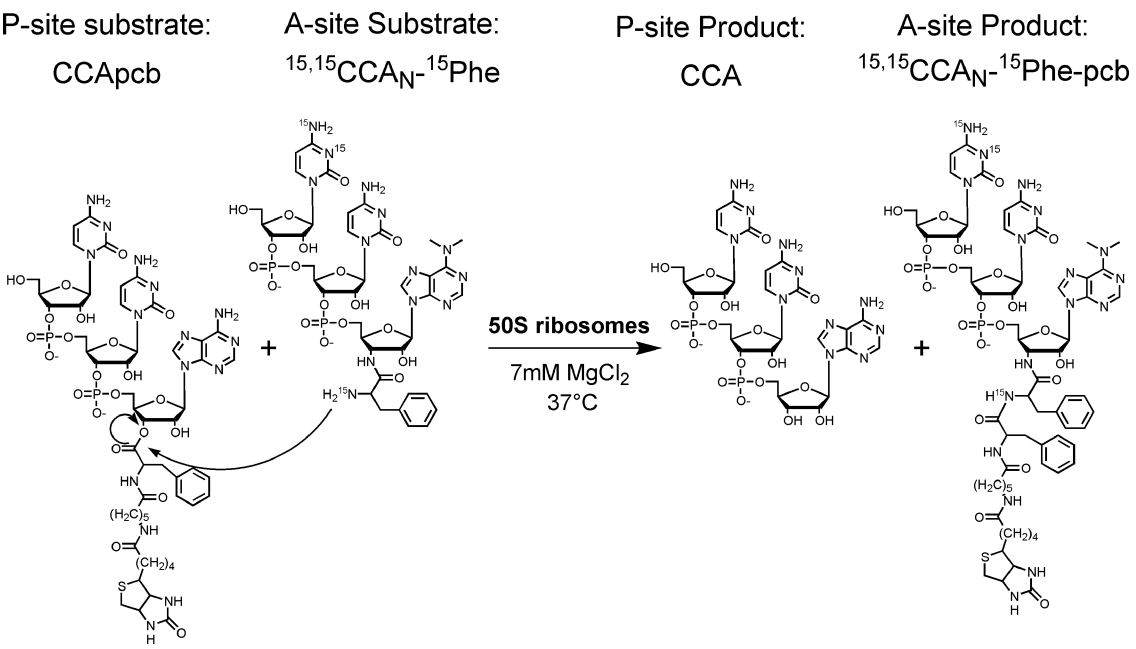

FIGURE 1: Schematic of the modified fragment assay. The substrates are on the left, and the products are on the right. $^{15,15}CCA_N$-^{15}Phe and CCApcb undergo a ribosome-dependent reaction in which a peptide bond is formed between the α-amino group of $^{15,15}CCA_N$-^{15}Phe and the carbonyl carbon of CCApcb. The products of the reaction are deacylated CCA and $^{15,15}CCA_N$-^{15}Phe-pcb. Substrate $^{15,15}CCA_N$-Phe and CCA_N-Phe are identical to $^{15,15}CCA_N$-^{15}Phe shown here except that the heavy-atom substitution is not present at the α-amino group of either of these substrates and CCA_N-Phe has no heavy atom substitutions. The 5′ cytidine and the penultimate cytidine mimic C74 and C75 of the tRNA, respectively.

is also not suitable for measuring KIEs. The translational cofactor EF-G mediates movement of the peptidyl tRNA into the ribosomal P site leading to complete commitment to catalysis, which would mask any KIEs on the chemical step for the P-site substrate. In principle, the isotope effect for the A-site substrate puromycin could be measured under pre-steady-state conditions, but generating sufficient material for mass spectroscopic analysis under these conditions would be prohibitive.

We anticipated that isotope effect measurements on the ribosome would be challenging because of the large size of both the enzyme (2.5 MDa) and its substrates; therefore, we selected a more simplified system for the analysis. Model reactions that simplify the mechanism have been used to measure KIEs on many enzymes (*15*−*19*). An ideal system for determining the KIE on peptide bond formation would include the following features: (i) the reaction coordinate must be simplified, and all steps prior to the chemical step must be completely reversible; (ii) the substrates must be small and amenable to chemical synthesis for incorporation of specific isotopic substitutions; and (iii) the reaction must be performed under multiple turnover reaction conditions to generate sufficient material for whole-molecule mass spectrometry analysis.

On the basis of these criteria, we developed a modified fragment assay in which 50S ribosomal subunits alone catalyze peptide bond formation between two small synthetic substrates that mimic the A- and P-site tRNAs (*20*). In this assay, cytidylyl-(3′-5′)-cytidylyl-(3′-5′)-N^6,N^6-dimethyl-adenosyl-3′-amino-3′-deoxy-3′-L-phenylalanine (CCA_N-Phe), an amide-linked puromycin derivative, and CCA-phenalanine-caproic acid-biotin (CCApcb) serve in place of the A- and P-site tRNA, respectively (Figure 1) (*21*). The α-amino group of CCA_N-Phe attacks the ester bond that links the phenylalanine-caproic acid-biotin with the CCA, to produce a new amide bond. Under single-turnover kinetic conditions, the reaction proceeds with a single-exponential decay approximately 300-fold slower than the 70S assay (*20*, *27*). Greater than 95% of the limiting substrate is converted to product (*21*). It appears that no steps are slower than the chemical step in the 50S assay based on two observations. Like the 70S assay, the reaction rate is highly dependent on pH and shows two acidity constant (pK_a) values in the reaction pH profile, both of which are within one pH unit of the values observed in the 70S assay (K. Okuda, A. C. Seila, and S. A. Strobel, manuscript submitted) (*14*). Second, when a hydroxyl is substituted for the α-amino group of puromycin, the reaction rate decreases 20- and 200-fold in the 50S and the 70S assays, respectively (A. C. Seila and S. A. Strobel, unpublished data) (*14*). This difference in aminolysis and alcoholysis rates is consistent with what is seen in the nonenzymatic reaction (*22*). Thus, this system appears to provide our best chance of successfully applying KIE analysis to the characterization of the ribosomal peptidyl transferase reaction.

In this paper, we establish a kinetic framework for using the modified fragment assay in KIE measurements. We determine whether substrate binding is random or ordered, and we measure both the forward and reverse commitments to catalysis. We then demonstrate the feasibility of the KIE approach for peptidyl transferase TS analysis by characterizing a heavy-atom nitrogen substitution at the A-site substrate α-amino group. A small normal isotope effect was observed at pH values both above and below the pK_a of the primary amine. The implications of this observation are discussed.

MATERIALS AND METHODS

Materials. CCApcb was synthesized by Dharmacon Research, Inc. The A-site substrate cytidylyl-(3′-5′)-3′-amino-3′-deoxy-3′-L-phenylalanyl-N^6,N^6-dimethyladenosine, CA_N-Phe, and CCA_N-Phe, are puromycin derivatives in which the *O*-methyl tyrosine is replaced with phenylalanine and the 5′ end has been extended by one or two cytidine nucleotide(s), respectively. $^{15,15}CCA_N$-^{15}Phe is an analogue of CCA_N-Phe that has two remote labels on the 5′ cytidine and one ^{15}N substitution at the α-amino group. $^{15,15}CCA_N$-Phe has two external labels on the 5′ cytidine but no ^{15}N substitution at the α-amino group. The ^{15}N remote labels are at the N3 position and the exocyclic amine of the C. All puromycin derivatives were prepared as described in Okuda et al. (*23*). All buffers and salts including MES, MOPS, Tris, sodium monophosphate, ammonium chloride, magnesium acetate, and magnesium chloride were purchased from Sigma/Aldrich Inc.

Preparation of 50S Ribosomal Subunits. 50S ribosomal subunits were isolated from *E. coli* strain MRE600 by a procedure modified from Lodmell et al. (*24*). A total of 20 g of cells was grown under forced aeration in a 10 L fermentor to a cell density of 0.8−0.9 A_{600} in liquid media containing 100 g of Tryptone-peptone, 50 g of yeast extract, and 100 g of NaCl. Bacteria were harvested by centrifuging at 7800*g* for 10 min. Cells were stored in 15−20 g aliquots at −80 °C.

The 50S ribosome subunits were prepared according to Rodnina and Wintermeyer, with the following modifications (*25*). The ribosomes were incubated in 20 mM Tris, 60 mM NH_4Cl, 5.25 mM MgOAc, 0.25 mM EDTA, and 3 mM 2-mercaptoethanol for >36 h to allow 70S dissociation into subunits before zonal centrifugation and collection of the 50S ribosomal peak. Ribosome concentrations were determined based on an extinction coefficient of 26.1 μM^{-1} cm^{-1}.

Initial Velocity Studies. Initial velocity studies were performed to determine if the reaction mechanism of the modified fragment reaction is random or ordered. All reactions were performed in 50 mM MOPS buffer at pH 7.0, 200 mM NH_4Cl, and 40 mM $MgCl_2$. All buffers were prepared as a 5× stock. CCApcb was 5′-^{32}P-end-labeled by phosphorylation with T4 polynucleotide kinase and [γ-^{32}P]-ATP. A total of 90 nM 50S subunits and unlabeled CA_N-Phe at varying concentrations in 1× buffer were incubated at 37 °C for 1 min prior to the start of the reaction. Variation of the incubation time at 37 °C (the ribosome activation step) from 1 to 10 min did not affect the overall reaction rate. In a separate tube, unlabeled CCApcb was mixed with trace 5′-^{32}P-radiolabeld CCApcb in 1× buffer. Substrate mix (2×) was added 1:1 to a 2× enzyme mix to begin the reaction. Aliquots were removed at specific intervals and quenched with 3 times the volume of Tris-MES FLB (90% formamide, 50 mM Tris-MES at pH 6.5, 0.04% bromophenol blue, and 0.04% xylene cyanol). The substrate and product were fractionated by electrophoresis into 12% acrylamide, 7 M urea, 50 mM Tris-NaH_2PO_4 at pH 6.5 gels, cooled to 4 °C. The substrate and product were quantitated by phosphorimager analysis on a Storm Imaging System 820 (Molecular Dynamics). The reaction rate (*k*) was determined by plotting the fraction of reacted substrate versus time using Kaleidagraph software and fit to the single-exponential curve, fraction reacted = $(0.97)(1 - e^{-(k+0.0013)t})$, where 0.97 is the reaction endpoint, 0.0013 is the background rate of hydrolysis for CCApcb, and *t* is time.

Experiments were performed at multiple concentrations of both CA_N-Phe and CCApcb to give a family of plots for each of the two substrates as described by Segal (*26*). The data were fitted to the Hanes−Woolf equation to distinguish a rapid equilibrium random mechanism from an ordered mechanism

$$\frac{[S]}{v} = \frac{1}{V_{max_{app}}}[S] + \frac{K_{M_{app}}}{V_{max_{app}}} \quad (1)$$

where [*S*] is the concentration of the varied substrate, v is the initial velocity, $K_{M_{app}}$ is the apparent Michaelis constant, and $V_{max_{app}}$ is the apparent maximal velocity. The initial velocity of the reactions at multiple concentrations of CA_N-Phe and CCApcb were measured to give a family of plots for both CA_N-Phe and CCApcb. The data were analyzed to determine if the reaction followed an ordered or random mechanism (*26*).

Forward Commitment to Catalysis. The forward commitment to catalysis for both CCA_N-Phe and CCApcb was determined using pulse-chase reactions. Reactions were performed in 25 mM MES, 25 mM MOPS, 50 mM Tris, 7 mM $MgCl_2$, 160 mM NH_4Cl at 37 °C. The MES, MOPS, and Tris (MMT) buffer system was chosen to allow for a wide pH range without having to control for buffer effects. In these experiments, CCA_N-Phe served as the A-site substrate. In the A-site substrate pulse-chase experiments, 9 μM 50S subunit, 130 μM CCApcb, and reaction buffer were incubated 2 min at 37 °C. Trace 5′-^{32}P-radiolabeled CCA_N-Phe was added to begin the reaction. At time t_1, which varied depending on the pH of the experiment, unlabeled CCA_N-Phe (chase) was added to give a final concentration of 1 mM. Samples were removed at intervals and quenched with 3 times the volume of FLB. Substrates were separated from products by electrophoresis on 12% acrylamide, 7 M urea, 100 mM Tris-borate-EDTA (TBE) gels. To determine the off rate for substrate binding, the "chased" reaction was compared to a reaction in which no chase was added.

Pulse-chase experiments for the P-site substrate were performed as follows: 9 μM 50S ribosomal and 900 μM CCA_N-Phe were incubated under the same conditions as the A-site substrate above. Trace 5′-^{32}P-radiolabeled CCApcb was added to begin the reaction. At 1 min, unlabeled CCApcb (chase) was added to give a final concentration of 900 μM. Samples were removed at intervals and quenched with 3 times the volume of Tris-MES FLB. Gel conditions were the same as in the initial velocity experiments above. Pulse-chase experiments for both CCA_N-Phe and CCApcb were performed at pH 5.2 and 8.5.

Reverse Commitment to Catalysis. The irreversibility of the reaction was established by incubating 50S ribosomal subunits with the products of the modified fragment assay, cytidylyl-(3′-5′)-cytidylyl-(3′-5′)-N^6,N^6-dimethyladenosyl-3′-amino-3′-deoxy-3′-L-phenylalanine-L-phenylalanine-caproic acid-biotin (CCA_N-Phe-pcb) and CCA. All reactions were performed in the buffer system described above for forward commitment studies. A total of 9 μM 50S subunits and unlabeled 0.5 mM CCA in 1× buffer were incubated at 37

°C for 1 min prior to the start of the reaction. 5′-^{32}P-end-labeled CCA_N-Phe-pcb was added to begin the reaction. Samples were removed at intervals and quenched in FLB (90% formamide, 0.04% bromophenol blue, and 0.04% xylene cyanol). The substrate was separated from the product by electrophoresis using 12% acrylamide, 7 M urea, 100 mM TBE gels.

Determination of KIEs by Electrospray Ionization Mass Spectrometry (ESI−MS). ^{15}N KIEs were determined for peptide bond formation using competitive methods and whole-molecule mass spectrometry. CCA_N-Phe and $^{15,15}CCA_N$-^{15}Phe were mixed in approximately equal amounts to give a pool of the A-site substrate. The isotopic composition of the initial substrate was determined by purifying 5 nmol of the A-site substrate (starting material) on an Agilent Technologies XBD-C_{18} reverse-phase HPLC column. A total of 10 mM triethylamine acetate (TEAA) at pH 6.5 was used as the mobile phase for all HPLC purifications. Substrates and products were separated by HPLC using a gradient of 0−30% acetonitrile over 30 min followed by an isocratic run for 10 min at 30% acetonitrile.

Experiments were performed to determine the change in the isotopic composition as the reaction progressed. The A-site substrate (20 nmol) was added to 30 nmol of CCApcb, MMT buffer, 7 mM $MgCl_2$, and 160 mM NH_4Cl at 37 °C. The 50S ribosomal subunits (4.5 μM) were added to begin the reaction. Once the reaction had proceeded to greater than 50% reacted, it was quenched by addition of ∼50 mM EDTA followed by HPLC purification and lysophilization under the same conditions as the starting material. The fraction reacted (f) was determined by dividing the area of the product peak (CCA_N-Phe-pcb) by the sum of the 2 peak areas, CCA_N-Phe and CCA_N-Phe-pcb.

Mass spectrometry was used to determine the isotopic composition of the initial substrate, $^{15}N_0/^{14}N_0$, and the substrate remaining after partial reaction, $^{15}N_r/^{14}N_r$. A-site substrate HPLC fractions for both the starting material and reaction were frozen and lyophilized to dryness. The purified A-site substrate was desalted by multiple rounds of lyophilization. Substrate $^{15}N/^{14}N$ ratios were analyzed on an Applied Biosystems PE SciEX API 3000 triple quadrupole mass spectrometer with an electrospray ion source (ESI−MS). For ESI−MS analysis, samples were resuspended in 1:1 10 mM TEAA/acetonitrile and injected by direct infusion at a rate of 10 μL/min. Single-ion monitoring was used to measure the ion intensities at the M (m/z 1050.3), M + 1 (m/z 1051.3), M + 2 (m/z 1052.3), M + 3 (m/z 1053.3), M + 4 (m/z 1054.3), and M + 5 (m/z 1055.3) peaks. The same procedure was used to determine the isotope effect due to the remote labels alone using a mixture of the substrates CCA_N-Phe and $^{15,15}CCA_N$-Phe. The $^{15}N/^{14}N$ ratio for the triple-labeled molecule ($^{15,15}CCA_N$-^{15}Phe/CCA_N-Phe) was computed by calculating the (M + 3)/M ratio, while the $^{15}N/^{14}N$ ratio for the double-labeled molecule ($^{15,15}CCA_N$-Phe/CCA_N-Phe) was computed by calculating the (M + 2)/M ratio.

Data Analysis. The ^{15}N isotope effect on the ribosomal reaction was measured using the internal competition method and whole-molecule mass spectrometry. Isotope effects measured by competitive methods can be determined from the change in the isotopic ratio of either the substrate or the product (*27*). When the substrate is analyzed, the relationship of the isotope effect to the isotopic composition is given by

$$ {}^{15}\left(\frac{V}{K}\right)^{-1} = \left(\frac{{}^{15}k}{{}^{14}k}\right) = \frac{\log\left(\dfrac{\dfrac{{}^{15}N_r}{{}^{14}N_r}}{\dfrac{{}^{15}N_0}{{}^{14}N_0}}\right)}{\log\left[(1-f)\dfrac{\left(1+\dfrac{{}^{15}N_0}{{}^{14}N_0}\right)}{\left(1+\dfrac{{}^{15}N_r}{{}^{14}N_r}\right)}\right]} + 1 \quad (2)$$

where $^{15}N_0/^{14}N_0$ is the isotopic composition of the substrate prior to the reaction, $^{15}N_r/^{14}N_r$ is the isotopic composition remaining after partial reaction, and f is the fraction reacted (*28*). Because heavy-atom KIEs are small (0−3%), the change in the isotopic ratios between $^{15}N_r/^{14}N_r$ and $^{15}N_0/^{14}N_0$ is also small (*12*). Increasing the fraction reacted increased the change in the ratio but also decreased the amount of material left for analysis of $^{15}N_r/^{14}N_r$. Whole-molecule mass spectrometry requires about 5 nmol of material, which precludes a high fraction reacted. Therefore, exact measurement of the precision in the substrate-starting and end-point ratios was critical.

Spectra were collected for an extended period of time (>15 min), providing a list of intensities with 500−1000 data points. $^{15}(V/K)$ was estimated using eq 2. At a low fraction reaction (<90%), the variance in $^{15}(V/K)$ is dominated by the variance in $\hat{\rho}$ (*29*).

$^{15}(V/K)$ was estimated using eq 2, where $^{15}N_r/^{14}N_r$ and $^{15}N_0/^{14}N_0$ were estimated using standard ratio estimation methods (*30*, *31*). Approximate estimators for the bias and the variance of $^{15}(V/K)$, which are valid for large samples, were derived from eq 2. Because the sample sizes were greater than 500, these estimators provided highly accurate estimates.

$^{15}(V/K)$ was determined for multiple reactions. The overall estimate of $^{15}(V/K)$ was obtained by averaging the individual sample ratio estimators. The estimate of the variance $^{15}(V/K)$ for all samples at a particular reaction condition, $\mathrm{Var}_{all}{}^{15}(V/K)$, was computed by

$$ \mathrm{Var}_{all}{}^{15}\left(\frac{V}{K}\right) = \frac{1}{n^2}\sum_{i=0}^{n}\mathrm{Var}^{15}\left(\frac{V}{K}\right) \quad (3)$$

From the experimentally determined values of the remote-label KIEs, $^{remote}(V/K)$, and the triple-label isotope effect, $^{\alpha,remote}(V/K)$, the effect due to heavy-atom substitution at the α-amino group was calculated according to eq 4, which assumes that the rule of the geometric mean holds (*32*, *33*).

$$ {}^{\alpha}(V/K) = \frac{{}^{\alpha,remote}(V/K)}{{}^{remote}(V/K)} \quad (4)$$

All calculations were performed using the software package R.[2] A more detailed description of the statistical procedure will be published separately.

[2] www.R-project.org.

TS Modeling. To understand the implications of the observed KIE on the TS structure, we performed a computational study utilizing a model aminolysis reaction that included ammonia, formic acid, and four water molecules. An in vacuo TS was determined at the density functional level [B3LYP/6-31+G(d,p)] using Gaussian 98's implementation of the synchronous transit-guided quasi-Newton method, using ammonia and formic acid as the starting molecules and the zwitterionic tetrahedral intermediate as the products (*34*, *35*). The ^{15}N isotope effect for this model TS was calculated at 298 K, from the Gaussian-derived force constants, using Isoeff98 (*36*).

We investigated the hypothesis that the ribosome utilizes general base catalysis to deprotonate the incoming nucleophile concomitantly with carbon−nitrogen bond formation by calculating the expected isotope effects for TS structures in which the nitrogen−hydrogen bond length is increased in a stepwise fashion. We applied a constraint to gradually separate the nitrogen and one hydrogen atom of the amine and reoptimized the TS structure for eight N−H distances ranging from 1.035 to 1.11 Å. KIEs were calculated for each of these new TS structures using Isoeff98 (*36*).

RESULTS

Determination of a Rapid Equilibrium Random Mechanism. The extent of bonding in the TS can be determined from the magnitude of the intrinsic isotope effect. The observed isotope effect for a competitive reaction has been defined by Northrop as

$$^{15}\left(\frac{V}{K}\right) = \frac{^{15}k + c_f + c_r K_{eq}}{1 + c_f + c_r} \quad (5)$$

where $^{15}(V/K)$ is the observed isotope effect, ^{15}k is the intrinsic isotope effect, c_f is the forward commitment to catalysis, c_r is the reverse commitment to catalysis, and K_{eq} is the equilibrium isotope effect (*37*). Determination of the commitment in both the forward and reverse directions is required to elucidate the relationship between the observed and intrinsic isotope effect. The kinetic experiments described below establish the framework for KIE studies on both the A- and P-site substrates.

The peptidyl transferase reaction was shown to be irreversible by incubating the modified fragment assay products with 50S ribosomal subunits. If k_{chem} for a given reaction is irreversible under the reaction conditions, then the observed isotope effect is independent of any rates or isotope effects for all steps following the chemical step (*37*). To test the reversibility of the 50S assay, products were incubated with 50S ribosomal subunits for as long as 6.5 h. No substrate was observed following this incubation, suggesting that the reverse reaction is negligible (data not shown). Although we cannot fully eliminate an on-enzyme reverse commitment, we expect that it is small because of the fast rate of product release.

Whether substrate binding is random or ordered defines how the KIE analysis is performed (*38*). During the elongation cycle of protein synthesis with full-sized tRNAs, substrate binding follows an ordered mechanism where the P-site tRNA is always bound before the A-site tRNA. To determine if the modified fragment assay follows a random

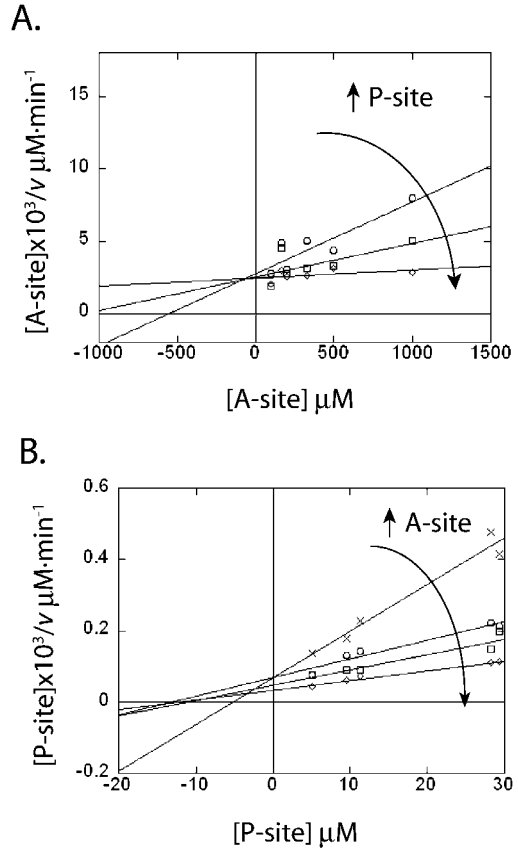

FIGURE 2: Kinetic parameters for peptide bond formation in the 50S ribosomal subunit. The substrate concentration dependence of [substrate]/v is presented in Hanes−Woolf plots. The x value at which the lines intersect gives the K_M value for that substrate. (A) Reaction rate was determined at varying concentrations of CA_N-Phe at multiple fixed concentrations of CCApcb, 5 μM (○), 9.5 μM (□), and 11.3 μM (◇). [CA_N-Phe] was divided by the reaction rate (v) and plotted against [CA_N-Phe]. (B) Reaction rate was determined at varying concentrations of CCApcb at multiple fixed concentrations of CA_N-Phe, 100 μM (○), 200 μM (□), 330 μM (◇), and 500 μM (×). [CCApcb] was divided by the reaction rate (v) and plotted against [CCApcb].

or ordered mechanism, K_M measurements for each of the two substrates were performed under multiple-turnover kinetic conditions. The A-site substrates, CCA_N-Phe and CA_N-Phe, have specificity for the ribosomal A site, while the P-site substrate, CCApcb, can bind both the ribosomal A and P sites (*21*). Initial velocity measurements were made under conditions in which the A- and P-site substrates are not saturating. This eliminates inhibition of the reaction by improper binding of CA_N-Phe to the ribosomal P site and CCApcb to the ribosomal A site. Initial rate measurements were made by varying the concentration of CA_N-Phe at multiple fixed concentrations of CCApcb.

Hanes−Woolf plots were used to determine if the substrates follow an ordered or random mechanism (*26*). The family of plots for both substrates intersect in the same quadrant, suggesting that the modified fragment reaction follows a rapid equilibrium random mechanism. When [CA_N-Phe] is varied at fixed concentrations of CCApcb, the family of plots cross in quadrant II (Figure 2A). When [CCApcb] is varied at multiple fixed concentrations of CA_N-Phe, the family of plots also intersect in quadrant II (Figure 2B). This suggests that the observed isotope effect will not decrease at high substrate concentrations, as would occur in an ordered

mechanism. These plots were not used to determine the K_M values for the two substrates because of the noise in the data, but under single-turnover conditions, the K_M for CA_N-Phe is 300 μM and the K_M for the enzyme when CCApcb is limiting is 3 μM (data not shown). The K_M of both substrates remains the same at 40 mM $MgCl_2$ and 7 mM $MgCl_2$, and it does not change as a function of pH. The values obtained from the multiple-turnover data are in agreement with the single-turnover K_M values. Product release is fast relative to the chemical step in the multiple-turnover reaction because the rate of peptidyl transferase under single- and multiple-turnover kinetic conditions is the same (data not shown).

The extent of forward commitment was determined for each substrate. The forward commitment for a reaction decreases the observed isotope effect and can be determined by pulse-chase experiments. The results for the A-site substrate CCA_N-Phe showed that the radioactive product does not form after chase addition. This indicates that the rate of substrate dissociation is fast relative to the slowest step of the reaction (Figure 3A). The results for CCApcb also show a very fast off rate for substrate binding with respect to the slowest step of the reaction (Figure 3B). Varying the reaction pH did not affect the substrate dissociation rate for either CCA_N-Phe or CCApcb (data not shown). This implies that at all pH values between 8.5 and 5.2 substrate binding to the 50S ribosomal subunit has a low-energy barrier for both CCA_N-Phe and CCApcb with respect to the chemical step-(s). These results are consistent with the relatively high K_M values for both substrates and the low k_{cat} of product formation ($\sim$3.8 min^{-1} at high pH) (*21*). Because both the forward commitment (c_f) and reverse commitment (c_r) are negligible, eq 11 simplifies to

$$^{15}\left(\frac{V}{K}\right) \approx {}^{15}k \qquad (6)$$

such that the observed KIE, $^{15}(V/K)$, can be considered the intrinsic KIE, ^{15}k. This establishes the utility of this system and these substrates for this type of detailed mechanistic analysis.

KIEs for Heavy-Atom Substitution at the α*-Amino Group of Puromycin.* The long-term goal of this analysis is to characterize the TS of the ribosome peptidyl transfer reaction using heavy-atom KIEs at multiple positions within both substrates. As a first step toward this goal, we studied the A-site substrate with a ^{15}N substitution at the nucleophilic α-amino group.

A potential difficulty in the determination of the isotope ratio is that the mass difference between CCA_N-Phe and CCA_N-^{15}Phe is only 1 Da. Because this substrate is large (exact mass = 1049.28), there is a substantial M + 1 peak because of natural abundance ^{13}C. The M + 1 peak intensity for this substrate is predicted to be 48% of the M peak. As expected, spectra of a mixture of CCA_N-Phe and CCA_N-^{15}Phe showed that the M + 1 peak due to the unlabeled substrate overlapped with the M peak arising from the labeled substrate. This made accurate ESI−MS analysis impossible. To avoid this overlap, we increased the mass difference between the heavy and light substrates. Two remote heavy-atom substitutions were incorporated in the ^{15}N-labeled substrate, in a manner reminiscent of the remote-labeling method (*27*, *33*, *39*) (Figure 1). The heavy-atom substitutions were incorporated into the 5′ cytidine C74, which does not participate directly in the chemical reaction and is not involved in hydrogen bonding to the ribosomal A site. Any effects that may arise from the presence of the remote labels were controlled for using a trinucleotide with only the external labels, $^{15,15}CCA_N$-Phe.

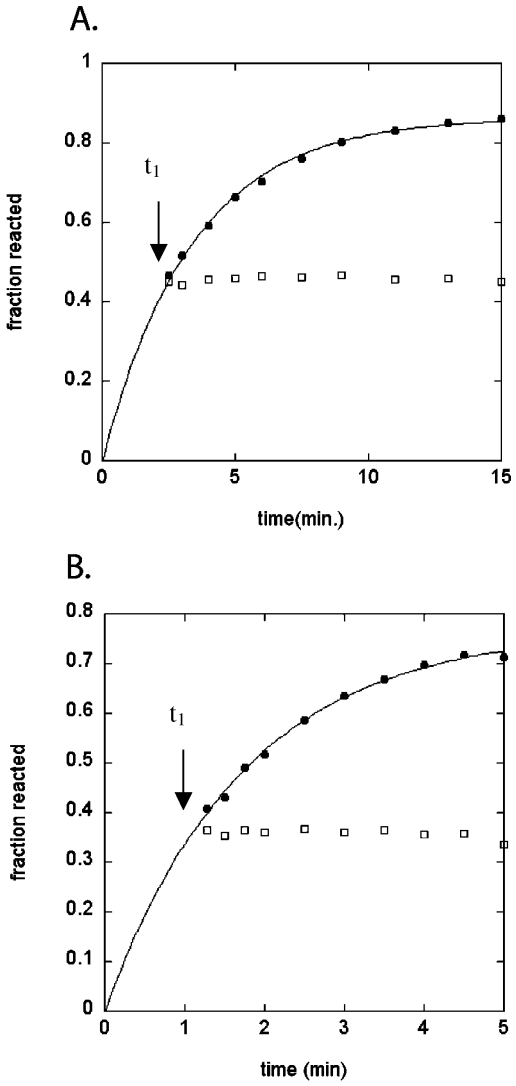

FIGURE 3: Forward commitment to catalysis of the 50S ribosomal subunit using pulse-chase experiments. (A) Fraction reacted versus time is shown for a reaction in which 10 μM 50S ribosomal subunits were combined with trace amounts of [5′-^{32}P]CCA_N-Phe. After 2 min, the reaction was diluted with 1 mM CCA_N-Phe (□) or allowed to proceed without chase (●). These data show that there is no significant forward commitment to catalysis. (B) Fraction reacted versus time is shown for a reaction in which 9 μM 50S ribosomal subunits were combined with trace amounts of [5′-^{32}P]CCApcb. After 1 min, the reaction was diluted with 0.9 mM CCApcb (□) or allowed to proceed without chase (●). These data suggest that the forward commitment for the P-site substrate, CCApcb, is negligible.

Utilizing this system, the KIE for ^{15}N substitution of the A-site nucleophile was determined at high pH (Table 1). The α-amino group of CCA_N-Phe has a pK_a of 6.9; therefore, a pH well above this value was selected to avoid complications arising from an equilibrium isotope effect due to deprotonation (*40*). At pH 8.5, the isotope effect for $^{15,15}CCA_N$-^{15}-Phe, $^{\alpha,remote}(V/K)$ was 1.0055 ± 0.0011. Dividing by the effect of the remote labels alone, $^{remote}(V/K)$, gives an $^{\alpha}(V/K)$ of 1.0097 ± 0.0012. At this pH, the α-amino group is

Table 1: ^{15}N Isotope Effects for the Ribosome as a Function of pH

pH	$^{\alpha,remote}(V/K)^a$	$^{remote}(V/K)^a$	$^{\alpha}(V/K)$	^{15}k
5.2	1.0155 ± 0.0023 (3)	0.9899 ± 0.0003 (3)	1.0259 ± 0.0039	1.0090
8.5	1.0055 ± 0.0011 (4)	0.9958 ± 0.0006 (4)	1.0097 ± 0.012	1.0097

[a] Number of determinations in parentheses.

deprotonated (*14*, *40*, *41*) and the observed isotope effect can be considered the intrinsic isotope effect [$^{15}(V/K) = {}^{15}k$], such that $^{15}k = 1.0097$. Thus, the isotope effect is normal and within the range expected for N^{15} substitution (0.97−1.03).

A normal ^{15}N isotope effect was also measured for the ribosome reaction at low pH (Table 1). At pH values below the pK_a of the α-amino group, most of the substrate will be protonated so

$$^{15}\left(\frac{V}{K}\right) = {}^{15}k(^{15}K_{eq}) \quad (7)$$

where $^{15}(V/K)$ is the observed isotope effect, ^{15}k is the intrinsic isotope effect, and $^{15}K_{eq}$ is the equilibrium isotope effect of proton dissociation. At pH 5.2, the isotope effect for $^{15,15}CCA_N$-^{15}Phe, $^{\alpha,remote}(V/K)$, was 1.0155 ± 0.0023. Dividing by the effect arising from the remote labels alone, $^{remote}(V/K)$, gives an $^{\alpha}(V/K)$ of 1.0259 ± 0.0039. As expected, the isotope effect increases as the pH is lowered, suggesting that the isotope effect, $^{15}(V/K)$, at low pH is due to both the equilibrium isotope effect ($^{15}K_{eq}$) and the intrinsic isotope effect (^{15}k). The equilibrium isotope effect on deprotonation of the puromycin α-amino group should be similar to the equilibrium isotope effect for phenylalanine, which was determined previously to be 1.0167 (*42*). Substituting this value into eq 8 gives $^{15}k = 1.0090$, the intrinsic isotope effect at pH 5.2. The difference in the intrinsic isotope effect at high and low pH is not statistically significant, but it is noteworthy that the intrinsic isotope effect is normal at both high and low pH.

TS Modeling. Although we have determined only the KIE for only one heavy-atom substitution, this value can still provide useful information to constrain possible models of the PT TS. Toward this goal, we performed a computational analysis of a model aminolysis reaction that included ammonia, formic acid, and four water molecules. In these calculations, we assumed that the reaction passes though a tetrahedral intermediate and performed in vacuo unrestrained optimizations of the reactant and tetrahedral intermediate structures.

The linear quadratic synchronous transit-guided quasi-Newton method was used to locate the TS, given the reactant and the tetrahedral intermediate as input structures. Vibrational analysis, performed at the same level of theory, showed a negative frequency (179 cm^{-1}) of normal mode vibration in the direction of the nucleophilic attack, validating this saddle point as the TS of the reaction under examination. The calculated ^{15}N KIE was found to be slightly normal (1.006), consistent with an early TS structure in which there is incomplete bond formation between the incoming nitrogen and the carbonyl carbon.

We also explored the hypothesis that the ribosome utilizes general base catalysis by strategically placing a base that could deprotonate the incoming nucleophile as the covalent bond is formed between nitrogen and carbon. We applied a constraint to gradually separate nitrogen and one hydrogen atom of the amine, mimicking the effect of a base pulling a proton from the amine, and reoptimized the TS structure for eight N−H distances, ranging from 1.035 to 1.11 Å. Once each new TS structure with the proton at the different N−H distances was located, ^{15}N KIEs were calculated. The results of the ^{15}N KIEs for the structures where the N−H distance was restrained showed a slight increase in the ^{15}N KIE as the N−H distance was elongated (at 1.11 Å, $^{15}k_{calc} = 1.009$). Therefore, deprotonation of the primary amine simultaneously with formation of the tetrahedral intermediate increases the observed isotope effect.

DISCUSSION

To measure KIEs on the ribosome, we developed and characterized the modified fragment assay (*21*). This peptidyl transferase assay utilizes two small substrates and 50S ribosomal subunits. The assay does not require the presence of mRNA, full size tRNAs, the 30S ribosomal subunit, organic cosolvent, or any GTP-dependent cofactors. Because there is no codon−anticodon interaction, accommodation is not rate-limiting. Both of the substrates are chemically synthesized, which makes them amenable to isotopic substitution at any position on either substrate. The reaction coordinate for this assay appears to consist of substrate binding, the chemical step, and product release. Because no factors are necessary for translocation, the modified fragment reaction can be performed under multiple turnover reaction conditions. We have determined that the 50S assay follows a rapid equilibrium random mechanism that the back reaction is negligible and that the forward commitment for both substrates is very small. This establishes that the observed KIEs reflect the chemical step(s) of the reaction, which makes the modified fragment assay well suited for TS analysis using isotopic substitutions within either the A- or P-site substrate.

As a first step toward characterizing the TS of the ribosomal peptidyl transferase reaction by KIE analysis, we measured the effect of isotopic substitution at the A-site substrate α-amino group by competitive methods and whole-molecule mass spectrometry, at two different pH values, one well below and one well above the pK_a of the α-amino group. Under both conditions, the isotope effect was normal (KIE = 0.9%) and equal within experimental error.

Nonenzymatic ester aminolysis reactions are predicted to proceed through a tetrahedral intermediate (*43*, *44*). Early studies by Jencks and co-workers showed that the aminolysis of methyl formate by many different amine nucleophiles proceeds via general base-catalyzed attack of free amine at high pH (Scheme 1) (*43*). As the reaction pH is lowered, there is a break in the pH profile, suggesting that there is a change in the rate-determining step of the reaction. At high pH, the amine attack step (k_1 in Scheme 1) is rapid and reversible and trapping of this intermediate by general base-

Scheme 1: Typical Aminolysis Reaction Mechanism

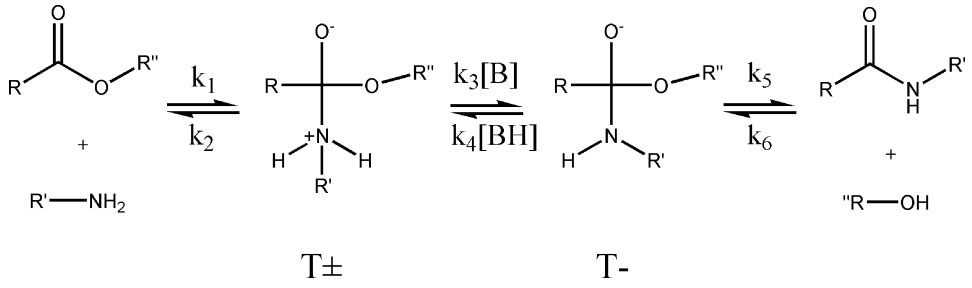

catalyzed proton removal or a proton switch through water ($k_3[B]$ in Scheme 1) is the rate-determining step (*44*). At low pH, the breakdown of the intermediate (k_5 in Scheme 1) is rate-determining (refs *43*−*47* and references therein).

When a reaction passes through an intermediate, the magnitude of the isotope effect (^{15}k) reflects isotope effects on the individual steps, as well as the relative rates of formation and decomposition of the intermediate (*48*). The isotope effect is defined by

$$^{15}k = \frac{\dfrac{^{15}k_1\,^{15}k_3\,^{15}k_5}{^{15}k_2\,^{15}k_4} + \dfrac{^{15}k_1\,^{15}k_3}{^{15}k_2}\left(\dfrac{k_5}{k_4[BH]}\right) + {}^{15}k_1\left(\dfrac{k_3k_5[B]}{k_2k_4[BH]}\right)}{1 + \dfrac{k_5}{k_4[BH]}\left(1 + \dfrac{k_3[B]}{k_2}\right)} \quad (8)$$

where the superscripts refer to the nitrogen isotope, and the subscripts refer to the steps as numbered in Scheme 1. If $k_3[B] \gg k_2$ in Scheme 1, the first irreversible step is k_1 and the observed ^{15}N isotope effect is $^{15}k_1$. If $k_5 \gg k_4[BH]$ and $k_3[B] \ll k_2$ in Scheme 1, k_3 is the first irreversible step and the observed ^{15}N isotope effect is $^{5}k_1{}^{15}k_3/{}^{15}k_2$. Last, if product release is faster than k_6, $k_5 \ll k_4[BH]$ and $k_2 \gg k_3[B]$ in Scheme 1, k_5 is the first irreversible step and the observed ^{15}N isotope effect is $^{15}k_1{}^{15}k_3{}^{15}k_5/{}^{15}k_2{}^{15}k_4$. If more than one step is partially irreversible, the observed isotope effect is a combination of the above expressions.

The 1.009 ^{15}N isotope effect for the ribosome reaction is consistent with a mechanism in which k_1 is the first irreversible step of the reaction, particularly if deprotonation of the primary amine was occurring at the same time as formation of the intermediate. On the basis of results from studies on the acylation of aniline, $^{15}k_1$ should be in the range of 1.004−1.000 (*48*). Computer modeling of the formation of the zwitterionic intermediate in the ammonia/formic acid model system minimized to an early TS in which there was incomplete N−C bond order. The calculated isotope effect for this TS is 1.006. Increasing the distance between the nitrogen and one proton increases the calculated isotope effect.

The observed KIE is inconsistent with other mechanistic possibilities. If in the ribosome reaction k_3 was the first irreversible step, then the isotope effect is predicted to be small and inverse, having a value of approximately 0.995. This estimate of the observed isotope effect for deprotonation of the zwitterionic intermediate, $^{15}k_1{}^{15}k_3/{}^{15}k_2$, is given by multiplying 1.0167, for deprotonation of phenylalanine, by 0.979, the equilibrium isotope effect on zwitterionic intermediate formation, $^{15}k_1/{}^{15}k_2$ (*42*, *48*). Therefore, the ribosomal ^{15}N isotope effect of 1.009 does not fit with a mechanism in which k_3 is the first irreversible step. An inverse isotope effect is also expected if k_5 is the first clearly irreversible step in the ribosome reaction. On the basis of the data available in the literature, the limiting value for $^{15}k_1{}^{15}k_3{}^{15}k_5/{}^{15}k_2{}^{15}k_4$, rate-limiting decomposition of the T$^-$ intermediate, is approximately 0.990, the measured isotope effect for aminolysis of methyl formate at pH 8 where breakdown of the T$^-$ intermediate is rate-limiting (ref *49* and below). Therefore, the ^{15}N isotope effect measured for the ribosome reaction suggests that the first irreversible step of the reaction is not the breakdown of the tetrahedral intermediate. If more than one step is partially irreversible, then the observed isotope effect will be somewhere between the limiting values of 1.009−0.990. Considering that the observed isotope effect is close to the upper limit, it is unlikely that multiple steps are contributing to the observed isotope effect, but this possibility cannot be excluded with the present data.

We also compared the incoming nucleophile isotope effect of the ribosome reaction to the isotope effect measured for two nonenzymatic ester-aminolysis model systems. Unlike the ribosome reaction, the nitrogen KIE for the acylation of aniline shows an inverse isotope effect of 0.996. The inverse isotope effect suggests that this reaction passes through a tetrahedral intermediate and that both formation of the tetrahedral intermediate and its breakdown are contributing to the reaction rate (*48*).

The ^{15}N KIE for nonenzymatic aminolysis of methyl formate by hydrazine has been measured at both high and low pH. The observed ^{15}N KIE is 0.992 at high pH and 0.990 at low pH (*49*). This is consistent with deprotonation of T±, $^{15}k_1{}^{15}k_3/{}^{15}k_2$, being the first irreversible at high pH and breakdown of the T$^-$ intermediate to products, $^{15}k_1{}^{15}k_3{}^{15}k_5/{}^{15}k_2{}^{15}k_4$, being the first irreversible step at low pH (*49*, *50*). Unlike the aminolysis of methyl formate, the 50S assay shows a normal intrinsic isotope effect at both high and low pH, inferring that the first irreversible step does not change as a function of pH.

The KIE is most consistent with a model in which formation of the tetrahedral intermediate is the first irreversible step of the reaction and deprotonation of the amine is occurring concurrently with intermediate formation. Consistent with this conclusion, the estimated Brönsted coefficient of the nucleophile for the peptidyl transferase reaction is less than 0.2, which suggests there is little charge development on the amine in the TS (*41*). This would occur if the increased N−C bond order was compenstated by the decreased N−H bond order. Thus, these two very different approaches to TS analysis appear to be arriving at a similar conclusion.

Whether the ribosome enhances the rate of peptide bond formation entirely by proper substrate positioning or by conventional chemical catalysis remains unresolved. Two catalytic strategies have been proposed to give rise to the $\sim 10^7$-fold rate enhancement for ribosomal peptide bond formation (for reviews, see refs *51*−*53*). The first is that the juxtaposition of the ester and amine by proper binding and positioning of the A- and P-site tRNA is the only catalytic contribution of the ribosome (*54*, *55*). The second hypothesis is that, in addition to substrate positioning, the ribosome utilizes general base catalysis by a strategically placed base in the active site (*14*). This base could deprotonate the incoming nucleophile as the covalent bond is formed between the nitrogen and carbon. The A76 2′ OH of the P-site tRNA has previously been suggested to serve this role in the ribosome reaction (*56*, *57*). The fact that the ^{15}N isotope effect for the ribosome reaction differs from that of a nonenzymatic aminolysis reaction suggests that proper substrate alignment is not the only catalytic contribution by the ribosome.

These results show that the 50S modified fragment assay is a valuable tool for understanding the mechanism of peptidyl transferase in the ribosome. We have successfully measured a KIE upon ^{15}N substitution at the nucleophilic amino group. This represents a rate effect resulting from a 1 Da change in molecular weight within a RNA−protein complex of ∼1.5 MDa. Although, this measurement gives no information on the extent of C_α−O bond cleavage at the TS, systematic analysis of isotope effects at positions on the P-site substrate will make it possible to completely characterize the TS of peptide bond formation.

ACKNOWLEDGMENT

The authors thank Dave Kitchen, Dharmacon Research, for assistance with solid-phase synthesis, Gerald Shulman and Anthony Romanelli for use of and assistance with mass spectrometry, Wallace Cleland, Vern Schramm, Karen Anderson, Adam Cassano, and Steve Ingalls for helpful discussions, and Jesse Cochrane and Rachel Anderson for helpful comments on the manuscript. We are especially grateful to one referee whose careful reading and detailed recommendations substantially improved the manuscript.

SUPPORTING INFORMATION AVAILABLE

PDB coordinates for the calculated structures of the modeling studies. This material is available free of charge via the Internet at http://pubs.acs.org.

REFERENCES

1. Pauling, L. (1946) *Chem. Eng. News*, 1375.
2. Melander, L., and Saunders, W. H., Jr. (1980) *Reaction Rates of Isotopic Molecules*, Wiley, New York.
3. (1978) *Transition States for Biochemical Processes*, Plenum Press, New York.
4. (1970) *Isotope Effects in Chemical Reactions*, Van Nostrand Reinhold, New York.
5. (1977) *Isotope Effects on Enzyme Catalyzed Reactions*, University Park Press, Baltimore, MD.
6. Schramm, V. L. (1999) Enzymatic transition-state analysis and transition-state analogs, *Methods Enzymol. 308*, 301−355.
7. Cleland, W. W. (1982) The use of isotope effects to determine transition-state structure for enzymatic reactions *Methods Enzymol. 87*, 625−641.
8. Cleland, W. W. (1982) Use of isotope effects to elucidate enzyme mechanisms, *CRC Crit. Rev. Biochem. 13*, 385−428.
9. Cleland, W. W. (1995) Isotope effects: Determination of enzyme transition state structure, *Methods Enzymol. 249*, 341−373.
10. Schramm, V. L. (1998) Enzymatic transition states and transition state analog design, *Annu. Rev. Biochem. 67*, 693−720.
11. Schramm, V. L. (2001) Transition state variation in enzymatic reactions, *Curr. Opin. Chem. Biol. 5*, 556−563.
12. O'Leary, M. H. (1980) Determination of heavy-atom isotope effects on enzyme-catalyzed reactions, *Methods Enzymol. 64*, 83−104.
13. Pape, T., Wintermeyer, W., and Rodnina, M. V. (1998) Complete kinetic mechanism of elongation factor Tu-dependent binding of aminoacyl-tRNA to the A site of the *E. coli* ribosome, *EMBO J. 17*, 7490−7497.
14. Katunin, V., Muth, G., Strobel, S., Wintermeyer, W., and Rodnina, M. (2002) Important contribution to catalysis of peptide bond formation by a single ionizing group within the ribosome, *Mol. Cell 10*, 339−346.
15. Rising, K. A. (1997) Transition state analysis of NAD^+ hydrolysis by cholera toxin catalytic subunit, *J. Am. Chem. Soc. 119*, 27−37.
16. Kline, P. C., and Schramm, V. L. (1993) Purine nucleoside phosphorylase. Catalytic mechanism and transition-state analysis of the arenolysis reaction, *Biochemistry 32*, 13212−13219.
17. Birck, M. R., and Schramm, V. L. (2004) Nucleophilic participation in the transition state for human thymidine phosphorylase, *J. Am. Chem. Soc. 126*, 2447−2453.
18. Berti, P. J., Blanke, S. R., and Schramm, V. L. (1997) Transition state structure for the hydrolysis of NAD^+ catalyzed by diphtheria toxin, *J. Am. Chem. Soc. 119*, 12079−12088.
19. Bahnson, B. J., and Anderson, V. E. (1991) Crotonase-catalyzed beta-elimination is concerted: A double isotope effect study, *Biochemistry 30*, 5894−5906.
20. Monro, R. E., and Marcker, K. A. (1967) Ribosome-catalysed reaction of puromycin with a formylmethionine-containing oligonucleotide, *J. Mol. Biol. 25*, 347−350.
21. Schmeing, T. M., Seila, A. C., Hansen, J. L., Freeborn, B., Soukup, J. K., Scaringe, S. A., Strobel, S. A., Moore, P. B., and Steitz, T. A. (2002) A pre-translocational intermediate in protein synthesis observed in crystals of enzymatically active 50S subunits, *Nat. Struct. Biol. 9*, 225−230.
22. Jencks, W. P., and Gilchrist, M. (1968) Nonlinear structure−reactivity correlations. The reactivity of nucleophilic reagents toward esters, *J. Am. Chem. Soc. 90*, 2622−2637.
23. Okuda, K., Seila, A. C., and Strobel, S. (2004) Synthesis of isotopically labeled puromycin derivatives for kinetic isotope effect analysis of ribosome catalyzed peptide bond formation, *Tetrahedron 60*, 12101−12112.
24. Lodmell, J. S., Tapprich, W. E., and Hill, W. E. (1993) Evidence for a conformational change in the exit site of the *Escherichia coli* ribosome upon tRNA binding, *Biochemistry 32*, 4067−4072.
25. Rodnina, M. V., and Wintermeyer, W. (1995) GTP consumption of elongation factor Tu during translation of heteropolymeric mRNAs, *Proc. Natl. Acad. Sci. U.S.A. 92*, 1945−1949.
26. Segal, I. H. (1993) *Enzyme Kinetics: Behavior and Analysis of Rapid Equilibrium and Steady-State Systems*, John Wiley and Sons, Inc., New York.
27. Oleary, M. H., and Marlier, J. F. (1979) Heavy-atom isotope effects on the alkaline-hydrolysis and hydrazinolysis of methyl benzoate, *J. Am. Chem. Soc. 101*, 3300−3306.
28. Bigeleisen, J., and Wolfsberg, M. (1958) Theoretical and experimantal aspects of isotope effects in chemical kinetics, *Adv. Biochem. Phys. 1*, 15−76.
29. Singleton, D. A., and Thomas, A. A. (1995) High-precision simultaneous determination of multiple small kinetic isotope effects at natural-abundance, *J. Am. Chem. Soc. 117*, 9357−9358.
30. Fishman, G. S. (1996) *Monte Carlo: Concepts, Algorithms, and Applications*, Springer-Verlag, New York.
31. van Kempen, G. M. P., and van Vliet, L. J. (2000) Mean and variance of ratio estimators used in fluorescence ratio imaging, *Cytometry 39*, 300−305.
32. Bigeleisen, J. (1955) Statistical mechanics of isotopic systems with small quantum corrections. 1. General considerations and the rule of the geometric mean, *J. Chem. Phys. 23*, 2264−2267.
33. Gawlita, E., Paneth, P., and Anderson, V. E. (1995) Equilibrium isotope effect on ternary complex formation of [1−18O]oxamate with NADH and lactate dehydrogenase, *Biochemistry 34*, 6050−6058.

34. Becke, A. D. (1993) Density-functional thermochemistry. III. The role of exact exchange, *J. Chem. Phys. 98*, 5648−5652.
35. Frisch, M. J., Trucks, G. W., Schlegel, H. B., Scuseria, G. E., Robb, M. A., Cheeseman, J. R., Zakrzewski, V. G., Montgomery, J. A., Stratmann, R. E., Burant, J. C., Dapprich, S., Millam, J. M., Daniels, A. D., Kudin, K. N., Strain, M. C., Farkas, O., Tomasi, J., Barone, V., Cossi, M., Cammi, R., Mennucci, B., Pomelli, C., Adamo, C., Clifford, S., Ochterski, J., Petersson, G. A., Ayala, P. Y., Cui, Q., Morokuma, K., Salvador, P., Dannenberg, J. J., Malick, D. K., Rabuck, A. D., Raghavachari, K., Foresman, J. B., Cioslowski, J., Ortiz, J. V., Baboul, A. G., Stefanov, B. B., Liu, G., Liashenko, A., Piskorz, P., Komaromi, I., Gomperts, R., Martin, R. L., Fox, D. J., Keith, T., Al-Laham, M. A., Peng, C. Y., Nanayakkara, A., Challacombe, M., Gill, P. M. W., Johnson, B., Chen, W., Wong, M. W., Andres, J. L., Gonzalez, C., Head-Gordon, M., Replogle, E. S., and Pople, J. A. (1998) *Gaussian 98*, Pittsburgh, PA.
36. Anisimov, V., and Paneth, P. (1999) Isoeff98. A program for studies of isotope effects using Hessian modifications, *J. Math. Chem. 26*, 75−86.
37. Northrop, D. B. (1981) The expression of isotope effects on enzyme-catalyzed reactions, *Annu. Rev. Biochem. 50*, 103−131.
38. Parmentier, L. E., Weiss, P. M., O'Leary, M. H., Schachman, H. K., and Cleland, W. W. (1992) ^{13}C and ^{15}N isotope effects as a probe of the chemical mechanism of *Escherichia coli* aspartate transcarbamylase, *Biochemistry 31*, 6570−6576.
39. Stoker, P. W., O'Leary, M. H., Boehlein, S. K., Schuster, S. M., and Richards, N. G. (1996) Probing the mechanism of nitrogen transfer in *Escherichia coli* asparagine synthetase by using heavy atom isotope effects, *Biochemistry 35*, 3024−3030.
40. Narula, S. S., and Dhingra, M. M. (1986) Determination of ionization sites and p*K* values in puromycin and puromycin aminonucleoside by C-13 and H-1 magnetic-resonance, *Indian J. Biochem. Biophys. 23*, 306−315.
41. Okuda, K., Seila, A. C., and Strobel, S. (2004) Uncovering the enzymatic pK_a of the ribosomal peptidyl transferase reaction utilizing a fluorinated puromycin derivative, manuscript submitted.
42. Hermes, J. D., Weiss, P. M., and Cleland, W. W. (1985) Use of N-15 and deuterium-isotope effects to determine the chemical mechanism of phenylalanine ammonia-lyase, *Biochemistry 24*, 2959−2967.
43. Blackburn, G. M., and Jencks, W. P. (1968) Mechanism of aminolysis of methyl formate, *J. Am. Chem. Soc. 90*, 2638−2645.
44. Satterthwait, A. C., and Jencks, W. P. (1974) Mechanism of aminolysis of acetate esters, *J. Am. Chem. Soc. 96*, 7018−7031.
45. Yang, C. C., and Jencks, W. P. (1988) The aminolysis of methyl formate with aniline−Evidence for catalysis by a trapping mechanism, *J. Am. Chem. Soc. 110*, 2972−2973.
46. Cox, M. M., and Jencks, W. P. (1981) Catalysis of the methoxyaminolysis of phenyl acetate by a preassociation mechanism with a solvent isotope effect maximum, *J. Am. Chem. Soc. 103*, 572−580.
47. Cox, M. M., and Jencks, W. P. (1981) Concerted bifunctional proton-transfer and general-base catalysis in the methoxyaminolysis of phenyl acetate, *J. Am. Chem. Soc. 103*, 580−587.
48. Kaminski, Z. J., Paneth, P., and Oleary, M. H. (1991) Nitrogen kinetic isotope effects on the acylation of aniline, *J. Org. Chem. 56*, 5716−5718.
49. Marlier, J. F., Haptonstall, B. A., Johnson, A. J., and Sacksteder, K. A. (1997) Heavy-atom isotope effects on the hydrazinolysis of methyl formate, *J. Am. Chem. Soc. 119*, 8838−8842.
50. Singleton, D. A., and Merrigan, S. R. (2000) Resolution of conflicting mechanistic observations in ester aminolysis. A warning on the qualitative prediction of isotope effects for reactive intermediates, *J. Am. Chem. Soc. 122*, 11035−11036.
51. Parnell, K. M., and Strobel, S. A. (2003) HIS and HERS, magic magnesium and the ballet of protein synthesis, *Curr. Opin. Chem. Biol. 7*, 528−533.
52. Green, R., and Lorsch, J. R. (2002) The path to perdition is paved with protons, *Cell 110*, 665−668.
53. Rodnina, M. V., and Wintermeyer, W. (2003) Peptide bond formation on the ribosome: Structure and mechanism, *Curr. Opin. Struct. Biol. 13*, 334−340.
54. Sievers, A., Beringer, M., Rodnina, M. V., and Wolfenden, R. (2004) The ribosome as an entropy trap, *Proc. Natl. Acad. Sci. U.S.A. 101*, 7897−7901.
55. Youngman, E. M., Brunelle, J. L., Kochaniak, A. B., and Green, R. (2004) The active site of the ribosome is composed of two layers of conserved nucleotides with distinct roles in Peptide bond formation and Peptide release, *Cell 117*, 589−599.
56. Weinger, J. S., Kitchen, D., Scaringe, S. A., Strobel, S. A., and Muth, G. W. (2004) Solid-phase synthesis and binding affinity of peptidyl transferase transition state mimics containing 2′-OH at P-site position A76, *Nucleic Acids Res. 32*, 1502−1511.
57. Dorner, S., Polacek, N., Schulmeister, U., Panuschka, C., and Barta, A. (2002) Molecular aspects of the ribosomal peptidyl transferase, *Biochem. Soc. Trans. 30*, 1131−1136.

BI047742F